



Evaluation of bacterial uptake, antibacterial efficacy against *Escherichia coli*, and cytotoxic effects of moxifloxacin-loaded solid lipid nanoparticles

Merve Eylül Kiyimaci¹, Gizem Ruya Topal², Ozgur Esim³, Merve Bacanlı⁴, Cansel Kose Ozkan³,
Onur Erdem⁴, Ayhan Savaser³, and Yalcin Ozkan³

¹ University of Health Sciences Turkey, Gülhane Faculty of Pharmacy, Department of Pharmaceutical Microbiology, Ankara, Turkey

² University of Health Sciences Turkey, Gülhane Faculty of Pharmacy, Department of Pharmaceutical Biotechnology, Ankara, Turkey

³ University of Health Sciences Turkey, Gülhane Faculty of Pharmacy, Department of Pharmaceutical Technology, Ankara, Turkey

⁴ University of Health Sciences Turkey, Gülhane Faculty of Pharmacy, Department of Pharmaceutical Toxicology, Ankara, Turkey

[Received in July 2022; Similarity Check in July 2022; Accepted in November 2022]

Moxifloxacin (MOX) is an important antibiotic commonly used in the treatment of recurrent *Escherichia coli* (*E. coli*) infections. The aim of this study was to investigate its antibacterial efficiency when used with solid lipid nanoparticles (SLNs) and nanostructured lipid carriers (NLCs) as delivery vehicles. For this purpose we designed two SLNs (SLN1 and SLN2) and two NLCs (NLC1 and NLC2) of different characteristics (particle size, size distribution, zeta potential, and encapsulation efficiency) and loaded them with MOX to determine its release, antibacterial activity against *E. coli*, and their cytotoxicity to the RAW 264.7 monocyte/macrophage-like cell line *in vitro*. With bacterial uptake of 57.29 %, SLN1 turned out to be significantly more effective than MOX given as standard solution, whereas SLN2, NLC1, and NLC2 formulations with respective bacterial uptakes of 50.74 %, 39.26 %, and 32.79 %, showed similar activity to standard MOX. Cytotoxicity testing did not reveal significant toxicity of nanoparticles, whether MOX-free or MOX-loaded, against RAW 264.7 cells. Our findings may show the way for a development of effective lipid carriers that reduce side effects and increase antibacterial treatment efficacy in view of the growing antibiotic resistance.

KEY WORDS: antibiotic; biocompatibility; drug resistance; *E. coli*; lipid-based nanoparticles; RAW 264.7 cell line

Resistance to antibiotics has become a serious healthcare issue as it erodes the efficiency of many currently used antibiotics (1–4). According to the World Health Organization (WHO), antimicrobial resistance is one of the most important dangers for people's health in the world and may become the cause of 10 million deaths every year by 2050 (5). New antimicrobial strategies are therefore needed to address this issue. In the fight against antibiotic resistance, new studies are focused on discovering and developing alternative agents like synthetic active ingredients (6), plant metabolites (7), antimicrobial peptides (8), virulence inhibitors (9), phages (10), and nanosized drug delivery technologies (11, 12). These include nanoparticles, which are carrier systems with a size of 10–1,000 nm in diameter, usually of natural or synthetic and biodegradable or non-biodegradable materials (13). In these systems, a drug can be dissolved, trapped, and/or encapsulated (14, 15) to achieve higher efficacy through higher uptake at lower risk of adverse effects (16).

Among them, lipid nanoparticles (LNPs) have gained popularity over the last few decades. Solid lipid nanoparticles (SLNs) consist of a solid lipid core stabilised by surfactants. Nanostructured lipid carriers (NLCs), are a step further from SLNs (16, 17), as they contain a mixture of solid and liquid lipids. Lipid particles have

many advantages over standard drug formulations because of their adaptability, low toxicity, high bioavailability, possibility to deliver both hydrophilic and lipophilic drugs, and easy scaling up that enables large-scale production (18–20).

Due to their lipophilic nature, SLNs and NLCs can also easily cross barriers like the bacterial cell membrane (21), and entrap hydrophobic drugs. Although some studies (22, 23) reported encapsulation of hydrophilic drugs as well, loading of a high amount of hydrophilic drugs in these carriers is more challenging and involves careful selection of solid or liquid lipids and suitable surfactants used in lipophilic and aqueous phases (24).

One such hydrophilic drug is moxifloxacin (MOX), a water-soluble fluoroquinolone derivative with broad-spectrum antibiotic activity. It inhibits the bacterial DNA gyrase and topoisomerase IV enzymes to disrupt DNA replication and repair and kill susceptible bacterial cells (25). It is used in the treatment of skin (26) and respiratory tract infections like chronic bronchitis, pneumonia, and acute bacterial sinusitis. It is especially effective against recurrent *Escherichia coli* (*E. coli*) infections (27, 28).

Loading an antibiotic into colloidal carriers like LNPs could counteract the efflux mechanism, through which resistance is

developed, and increase intracellular retention of the drug (29). Wong et al. (30) encapsulated ciprofloxacin, which belongs to the same antibiotic family as MOX, in multilamellar liposome vesicles to improve its *in vivo* activity against *Francisella tularensis* and *Brucella melitensis*. However, as far as we know, MOX has not been studied in this context so far. The aim of our study was to find a way to enhance its uptake into bacterial cell using these lipid carrier systems, as they structurally resemble the bacterial membrane. We also wanted to see if lower antibiotic concentration could maintain the efficiency of a standard treatment dose of MOX. We also characterised the nanoparticles in terms of their size, distribution, zeta potential, encapsulation efficiency, and *in vitro* release. To determine the biocompatibility of the newly developed formulations, we also investigated the cytotoxic effects of LNPs in RAW 264.7 monocyte/macrophage-like cells.

MATERIALS AND METHODS

Glyceryl dibehenate (CAS Nos. 6916-74-1, 77538-19-3, 30233-64-8; brand name Compritol® 888 ATO), serving as solid lipid, was a gift from Gattefossé-SAS (Saint-Priest, France). Poloxamer 407, Tween (polysorbate) 80, triethanolamine (TEA), and fluorescein were bought from Sigma (Munich, Germany). MOX was a gift from Koçak Farma (Istanbul, Turkey). Docosahexanoic acid (DHA) (CAS No. 6217-54-5) and oleic acid (CAS No. 112-80-1), serving as liquid lipids, were kindly provided by Croda Inc. (New Jersey, NJ, USA). In addition, bacterial media, namely tryptic soy agar (TSA; agar 15 g/L, casein peptone 15 g/L, sodium chloride 5 g/L, soy peptone 5 g/L) and tryptic soy broth (TSB; casein peptone 17 g/L, dipotassium hydrogen phosphate 2.5 g/L, glucose 2.5 g/L, sodium chloride 5 g/L, soya peptone 3 g/L) used for growing the bacteria and Mueller Hinton agar (MHA; agar 17 g/L, beef infusion solids 2 g/L, casein hydrolysate 17.5 g/L, starch 1.5 g/L) and cation-adjusted Mueller Hinton broth (MHB; acid hydrolysate of casein 17.5 g/L, beef extract 3 g/L, starch 1.5 g/L) used for antibacterial activity tests were purchased from Merck Life Science (Darmstadt, Germany). All the other chemicals were of analytical grade.

Chemicals used for cytotoxicity testing were purchased from the following suppliers: Dulbecco's Modified Eagle Medium (DMEM) and Dulbecco's Phosphate-Buffered Saline (PBS) from Wisent Bioproducts (Quebec, Canada), trypsin-EDTA from

Biological Industries (Beit-Haemek, Israel), foetal bovine serum (FBS) and penicillin-streptomycin from Capricorn Scientific (Ebsdorfergrund, Germany), and dimethyl sulphoxide (DMSO) and 2,2-diphenyl-1-picrylhydrazyl (DPPH) from Sigma-Aldrich Chemicals (Munich, Germany).

E. coli ATCC 25922 were obtained from the American Type Culture Collection (ATCC).

The RAW 264.7 monocyte/macrophage-like cells were kindly provided by Yeditepe University Faculty of Pharmacy, Department of Pharmaceutical Toxicology, İstanbul, Turkey.

Preparation of lipid nanoparticles

SLNs and NLCs were prepared by ultrasonication (31) using components reported in Table 1. For SLNs we used only solid lipids in the lipid phase. Lipids were first melted and heated to 70 °C with Tween 80 or poloxamer 407 used as emulsifiers. Then we heated 10 mL of water containing 10 mg of MOX to 70 °C and added to the lipid phase. The mixture was sonicated with a probe sonicator (Sonopuls, Bandelin, Germany) at 50 % amplitude for 1 min and let to cool down to room temperature (25 °C) for 2 h to allow formation of particles. A similar method was used to obtain the NLCs, except that solid and liquid lipids were combined as the lipid phase (see Table 1 for details). Moreover, blank nanoparticles (without MOX) were prepared to compare the effects.

To label the nanoparticles, fluorescein (5 mg) was added instead of MOX at the lipid phase step and mixed with magnetic stirrer for 30 s. The water phase and the remaining steps were applied as described above.

Determination of particle size, polydispersity index, and zeta potential

Nanoparticle size and polydispersity index (PDI) were measured with photon correlation spectroscopy (aka dynamic light scattering) and zeta potential with laser Doppler velocimetry (both using the Nicomp Nano Z3000 system, PSS, Inc., New York, NY, USA). Each sample was measured in triplicate (32).

Encapsulation efficiency (EE)

To calculate loaded MOX we used an indirect method by measuring MOX content in supernatants. Samples were centrifuged

Table 1 Composition of lipid nanoparticles

Formulation code	Solid lipid (glyceryl dibehenate)	Liquid lipid (docosahexanoic acid, DHA)	Liquid lipid (oleic acid)	Tween 80	Poloxamer 407	Triethanolamine (TEA)
SLN1	150 mg	-	-	100 mg	-	-
SLN2	150 mg	-	-	-	100 mg	-
NLC1	110 mg	40 mg	10 mg	-	100 mg	10 mg
NLC2	110 mg	40 mg	-	-	100 mg	10 mg

NLC – nanostructured lipid carrier; SLN – solid lipid nanoparticle

(IEC Centra MP4R, Rockville, USA) at 9000 *g* for 20 min and MOX detected with a high performance liquid chromatograph (HPLC, Agilent 1260 Infinity, Agilent Technologies Inc., Waldbronn, Germany) using a C18 column (150 mm × 4.6 mm i.d., 5 μm; ACE, Reading, UK) at the wavelength of 302 nm. Column temperature was 30 °C. The mobile phase was a mix of methanol-distilled water-acetonitrile (60:45:5) (v/v/v). It was adjusted to pH 2.7 with o-phosphoric acid. The flow rate was 1 mL/min (33).

In vitro drug release studies

MOX release from the nanoparticles was determined with the dialysis bag method (34). One millilitre (1 mL) of each nanoparticle suspension was placed in a dialysis bag (12–14 kDa, Spectrum Labs, USA) and the bag immersed in 50 mL of PBS (pH 7.4) and held in a shaker (Nuve, Istanbul, Turkey) operating at 50 rpm at 37 °C. MOX release was determined in 1 mL of PBS taken out from the pool at 15 and 30 min, and 1, 2, 4, 6, 8, 12, and 24 h. After each reading the PBS buffer was replaced with the same volume of a fresh one. The amount of released MOX was measured with the Agilent HPLC mentioned above.

TEM analysis

To characterise the morphology of MOX-loaded SLNs and NLCs, the particles were observed under a FEI Tecnai G2 Spirit BioTwin (Thermo Fisher, Waltham, MA, USA) transmission electron microscope (TEM) operating at 40 kV and 80,000× magnification. Samples were mounted on copper grids with a mesh size of 200 (75 microns), stained with 2 % uranyl acetate for 2 min, and then the excess removed with filter paper. The remainder was dried in a Petri dish for 2 h before microscopy.

Stability tests

Vials with formulations were kept in a dark fridge at +4 °C for one month and their particle size, polydispersity index, and zeta potential rechecked as described above.

Bacteria

E. coli ATCC 25922 were cultivated in tryptic soy agar and tryptic soy broth at 35±1 °C, and the study was carried out with 24-hour fresh bacterial cultures.

Bacterial uptake of nanoparticles

To determine the bacterial uptake of SLNs and NLCs we used fluorescent microscopy and flow cytometry. Briefly, 0.1 mL of *E. coli* suspension at log phase was added to SLNs and NLCs and incubated at 37 °C for 2 h. After incubation, the bacterial pellet and culture supernatant were separated by centrifugation at 4137 *g*. The pellet was washed with sterile distilled water three times to discard free NLCs or SLNs and then resuspended in 1 mL of sterile distilled water. The fluorescent intensity of *E. coli* cells was observed with a

CYTOFlex cytometer (Beckman Coulter, Suzhou, China). Blue fluorescence was collected through a 525/40 BP fluorescent channel with a 488 nm blocking filter. For each sample around ten thousand cells were analysed. Data were measured and histograms created and interpreted using the CytExpert 2.4 Software (Beckman Coulter, Indianapolis, IN, USA). In addition, to detect the position of MOX-loaded NLCs and SLNs in bacteria, the cells were observed under a DMIL inverted fluorescent microscope at 40× magnification and images taken (Leica, Munich, Germany).

Antibacterial activity

Antibacterial activity against *E. coli* was tested with the broth microdilution method for minimal inhibition concentration (MIC) and with the disc diffusion test for the inhibition zone according to the European Committee on Antimicrobial Susceptibility Testing standards (35). For the disc diffusion test we used 4.0±0.5 mm deep Mueller-Hinton agar plates (25 mL in a 90 mm circular Petri dish). Bacterial suspensions were prepared from fresh *E. coli* cultures in sterile saline (0.9 % NaCl) to the density of a 0.5 McFarland measured with a DEN-1B densitometer (Biosan SIA, Riga, Latvia). A sterile cotton swab was dipped into bacterial suspensions and spread on the agar surface in three directions. Discs with MOX-loaded SLNs and NLCs were then placed on the surface of inoculated agar plates and incubated at 35±1 °C for 18±2 h. After incubation, inhibition diameters around the discs were measured and compared to standard MOX as control.

For the broth microdilution (MIC) test 100 μL of cation-adjusted Mueller-Hinton broth added to all U-bottom microplate wells. We added 100 μL of MOX-loaded nanoparticle solution to the first well and diluted it further across 12 wells. Then the bacterial suspension (in saline, 0.9 % NaCl) with the density of the 0.5 McFarland (1×10⁸ CFU/mL) was 1:100 diluted and added to all wells to obtain the final bacterial concentration of 5×10⁵ CFU/mL. The microplates were then incubated at 35±1 °C for 18±2 h, and MIC determined as the lowest concentration of MOX-loaded SLN and NLC solutions that visibly inhibited the growth of *E. coli*.

Preparation of RAW 264.7 cell cultures

RAW 264.7 cells were seeded in 25 cm² flasks filled with 7 mL of DMEM supplemented with 10 % FBS, and 1 % penicillin-streptomycin and then grown in an incubator (Sanyo, Osaka, Japan) at 37 °C in an atmosphere supplemented with 5 % CO₂ for 24 h.

Cytotoxicity assay

Cytotoxicity was determined with the 3-(4,5-dimethylthiazol-2-yl)-2,5-diphenyltetrazolium bromide (MTT) assay as described earlier by Bacanli et al. (36). Cells were detached with a cell scraper and a total of 10⁵ cells/well seeded in 96-well tissue-culture plates. The cells were incubated in full medium with various concentrations (0.010, 0.025, 0.05, and 0.1 μg/mL) of MOX alone, MOX-free SLNs, MOX-loaded SLNs, MOX-free NLCs, and MOX-loaded

NLCs at 37 °C in an atmosphere supplemented with 5 % CO₂ for 24, 48, and 72 h. For negative control we used a medium containing 10 % FBS and 1 % penicillin-streptomycin. After exposure, the medium was aspirated, cells washed with PBS, 10 µL of MTT (5 mg/mL of stock solution with PBS) added to 100 µL of cell suspension per well, and cells incubated for another 3 h. The MTT dye was then carefully removed and 100 µL of DMSO added to each well. The absorbance of each well was measured with a microplate reader (Epoch, BioTek Instruments, Winooski, VT, USA) at 570 nm.

Statistical analysis

For statistical analysis we used the SPSS for Windows v. 20.0 software (IBM, New York, NY USA). All data are expressed as means ± standard deviations of measurements in three biological replicates. As the distribution was normal, differences between the groups were compared using Student's *t* test. Statistical significance was set to $p < 0.05$.

RESULTS AND DISCUSSION

Lipid nanoparticle properties

The composition of lipid nanoparticles is given in Table 1. Visual inspection did not reveal any separation between the oil and water phase in the MOX-loaded SLNs and NLCs, that is, emulsification was successful.

We aimed for small particles for better uptake by bacteria. SLN1, which contains Tween 80 as emulsifier, had significantly lower particle size and PDI compared to SLN2, which contains poloxamer 407 ($p < 0.05$, Table 2). These differences in particle size and PDI are likely owed to the lower molecular weight of Tween 80 than that of poloxamer 407 (37), as suggested by similar studies (38, 39). PDI

values of SLNs were below 0.3 characteristic of a monodisperse system (40). SLN1 had lower encapsulation efficiency than SLN2, which may be related to its lower particle size. Zeta potentials were significantly different ($p < 0.05$), possibly due to different emulsifiers used in the SLNs.

NLC1 had bigger particles and distribution than NLC2. As known, particle size and distribution can be modified with sonication, which breaks coarse emulsion droplets to form a nano-emulsion, so it is one of important parameters to bear in mind while preparing lipid nanoparticles (41). If sonication is less effective, nanoparticles containing more liquid lipids, like NLC1, tend to form bigger particles, as liquid lipids increase the viscosity of coarse formulations.

Zeta potential of formulations may differ as particles contain different liquid phases. For instance, oleic acid, which was used in NLC2 as liquid phase, could shift the zeta potential from -6.3 ± 0.38 to -11.6 ± 0.61 . However, there was no significant difference in encapsulation efficiency between NLCs (Table 2).

Table 3 shows that there were no significant changes in particle size, polydispersity index, and zeta potential measured in the formulations after one month, save for the drop in zeta potential in the SLN1 formulation. However, it is clear that particles tend to aggregate during storage, which leads to a gain in size and polydispersity index and loss in zeta potential.

TEM images and photon correlation spectroscopy of LNPs show spherical particles of similar size (Figure 1).

Drug release

Figure 2 shows MOX release from nanoparticles. The release of standard (not nanoparticle-loaded) MOX was high in the first two hours, after which it kept dropping by the end of hour 4, at which point 95 % of MOX was released, and no more drug was

Table 2 Lipid nanoparticle properties

LNP	Particle size (nm)	Polydispersity index	Zeta potential (mV)	Encapsulation efficiency (%)
SLN1	181.6±1.27	0.25±0.02	-14.6±0.32	68.61±0.20
SLN2	201.8±1.65	0.29±0.02	-17.5±0.14	74.53±0.34
NLC1	176.8±1.90	0.57±0.23	-11.6±0.61	77.82±0.21
NLC2	132.4±1.62	0.51±0.53	-6.3±0.38	77.17±0.21

Results are represented as means ± standard deviations

Table 3 Stability of lipid nanoparticles stored for one month at +4 °C

Type of LNPs	Particle size (nm)		Polydispersity index		Zeta potential (mV)	
	Baseline value	After one month storage	Baseline value	After one month storage	Baseline value	After one month storage
SLN1	181.6±1.27	186.1±2.89	0.25±0.02	0.36±0.25	-14.6±0.32	-10.0±0.51*
SLN2	201.8±1.65	200.5±3.56	0.29±0.02	0.39±0.12	-17.5±0.14	-11.5±0.45*
NLC1	176.8±1.90	180.3±1.64	0.57±0.23	0.60±0.46	-11.6±0.61	-8.30±0.78
NLC2	132.4±1.62	135.2±3.98	0.51±0.53	0.65±0.22	-6.3±0.38	-5.62±0.96

Results are represent as means ± standard deviations. * significant difference from baseline ($p < 0.05$)

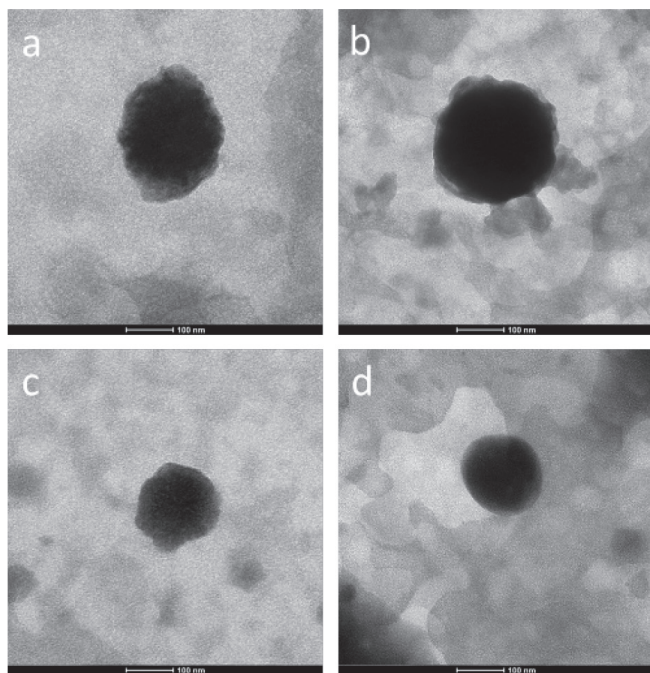


Figure 1 TEM images of SLN1 (a), SLN2 (b), NLC1 (c), and NLC2 (d) until hour 24. LNPs slowed down its release thanks to its even dispersion in the lipid matrix and diffusion from it, as previously proposed by other authors (42, 43).

Bacterial uptake of nanoparticles

Figure 3 shows flow cytometry findings of *E. coli* cells. There is no fluorescence signal in control cells (Figure 3a), which were incubated with unlabelled nanoparticles, whereas the rest shows a

strong signal (Figure 3b-f). Bacterial uptake of SLN1 and SLN2 (57.29 % and 50.74 %, respectively) was significantly more efficient than that of fluorescein solution alone (21.47 %) or either NLC (39.26 % for NLC1 and 32.79 % for NLC2) ($p < 0.05$).

Judging by higher uptake of lipid nanoparticles than the fluorescein solution alone, drug encapsulation in nanoparticles should enhance drug absorption owing to the small size, prolonged release, and hydrophobic nature of lipid nanoparticles, which is similar to the Gram-negative bacterial cell wall (44). Apparently, smaller size of SLN1 is also the reason for higher bacterial uptake than that of SLN2, which is in line with previous reports (45).

These findings are confirmed by fluorescence microscopy (Figure 4), as only a small number of bacterial cells absorbed fluorescein solution alone (Figure 4a), whereas lipid nanoparticles show better absorption (Figure 4b-e) and therefore confirm that they can better enter bacteria than the free drug, as suggested in a related study (14).

Antibacterial activity

Table 4 shows the antibacterial activity of nanoparticles in terms of inhibition zone (diameter) and MIC. Only the SLN1 formulation was significantly more effective against *E. coli* (MIC 0.020 $\mu\text{g}/\text{mL}$, 34 mm) than MOX delivered as a standard solution ($p < 0.05$). The NLC1 formulation showed better inhibition diameter (36 mm) than standard MOX but not MIC. In fact, SLN2 and both NLC formulations showed the same MIC as the corresponding standard MOX.

We know that *E. coli* with its thinner peptidoglycan layer and an outer lipopolysaccharide membrane has a limited permeability to drugs (46). Nanostructure with controlled drug release weakens its

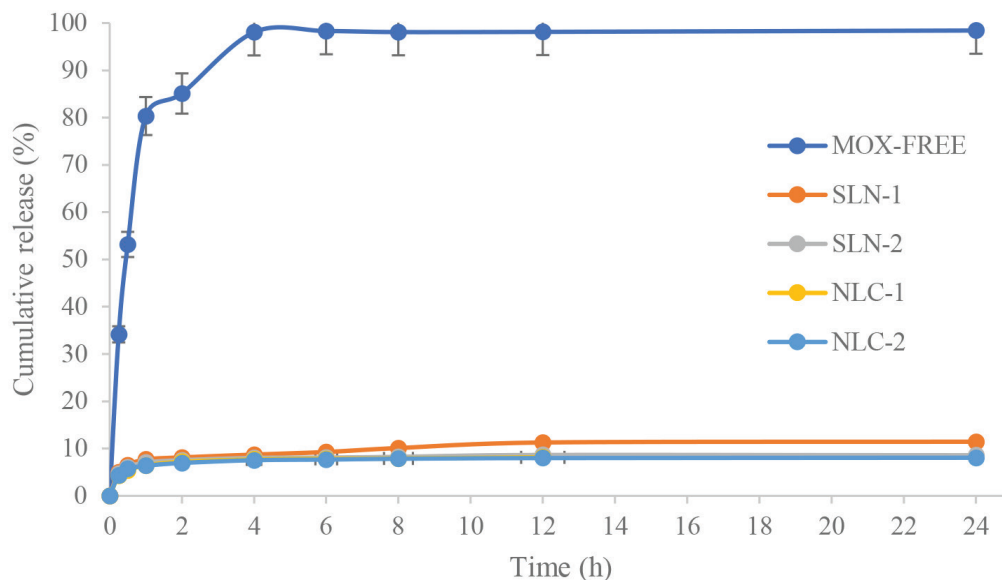


Figure 2 MOX release from nanoparticles

Table 4 Antibacterial activity of MOX-loaded SLNs and NLCs

Formulations	Inhibition diameter (mm)	Minimal inhibition concentration ($\mu\text{g/mL}$)
Standard MOX solution for SLNs * (0.68 mg)	33 \pm 0.07	0.041
SLN1	34\pm0.10***	0.020
SLN2	32 \pm 0.11	0.041
Standard MOX solution for NLCs** (0.78 mg)	35 \pm 0.08	0.023
NLC1	36 \pm 0.12	0.023
NLC2	35 \pm 0.05	0.023

*The concentration was equal to the amount of MOX loaded into SLNs. **The concentration was equal to the amount of MOX loaded into NLCs.

*** significant difference $p < 0.05$

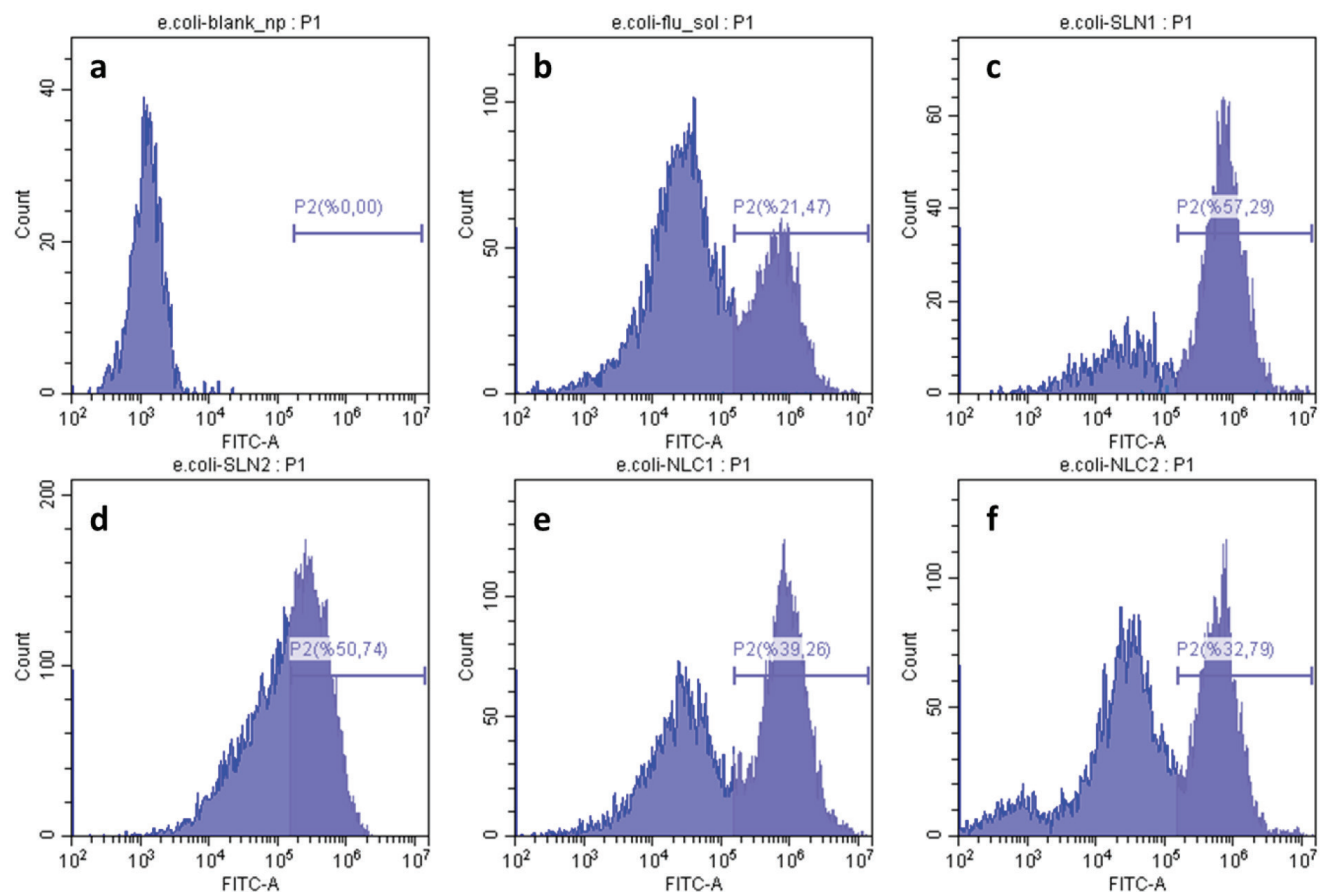


Figure 3 Flow cytometry results (a: blank NPS; b: fluorescein solution; c: SLN1; d: SLN2; e: NLC1; f: NLC2)

Table 5 Cytotoxic effects of MOX, MOX-free, and MOX-loaded LNPs in RAW 264.7 cells

	RAW 264.7 cell viability (%)											
	24 h				48 h				72 h			
	0.010 µg/mL	0.025 µg/mL	0.05 µg/mL	0.1 µg/mL	0.010 µg/mL	0.025 µg/mL	0.05 µg/mL	0.1 µg/mL	0.010 µg/mL	0.025 µg/mL	0.05 µg/mL	0.1 µg/mL
MOX	88.65±0.09	69.05±0.35	56.48±0.01	43.90±0.03	89.42±0.02	73.98±0.33	59.43±0.02	40.01±0.10	86.62±0.23	83.49±0.08	54.58±0.02	31.93±0.11
SLN1+MOX	81.56±0.26	75.43±0.29	75.92±0.23	74.55±0.23	94.62±0.02	81.95±0.11	71.44±0.03	58.43±0.06	92.13±0.08	91.46±0.34	89.06±0.28	73.70±0.22
SLN1	95.30±0.08	68.91±0.12	62.78±0.25	57.75±0.01	95.75±0.29	91.22±0.05	85.44±0.06	64.09±0.03	87.12±0.27	82.65±0.09	73.35±0.11	69.72±0.17
SLN2+MOX	93.14±0.08	80.42±0.19	66.66±0.46	62.10±0.21	88.73±0.06	77.09±0.12	63.16±0.12	56.05±0.04	92.13±0.08	91.46±0.34	89.06±0.28	73.71±0.22
SLN2	90.98±0.30	86.81±0.12	64.91±0.09	60.60±0.31	96.51±0.22	94.42±0.12	80.82±0.08	68.49±0.22	96.02±0.33	87.31±0.27	69.95±0.09	55.88±0.06
NLC1+MOX	80.46±0.09	81.65±0.18	85.84±0.26	81.47±0.09	88.72±0.09	72.27±0.04	62.23±0.02	51.10±0.15	85.24±0.09	76.56±0.30	73.78±0.09	56.03±0.32
NLC1	89.19±0.13	78.75±0.17	70.83±0.33	53.27±0.04	92.75±0.13	82.93±0.04	63.82±0.09	54.44±0.05	89.70±0.09	80.44±0.08	63.51±0.35	54.76±0.20
NLC2+MOX	78.43±0.31	65.99±0.05	56.58±0.29	50.72±0.04	76.23±0.27	59.40±0.03	53.59±0.06	53.05±0.08	94.10±0.27	79.09±0.03	73.90±0.06	51.68±0.17
NLC2	85.54±0.07	60.58±0.10	56.67±0.26	50.07±0.16	83.62±0.06	62.94±0.12	54.81±0.05	52.27±0.04	91.99±0.42	82.25±0.12	74.99±0.05	54.11±0.09

Results were given as means ± standard deviations

membrane resistance and increases drug uptake over time. In this sense, our findings are consistent with the ceftriaxone study by Kumar et al. (47).

We believe that the higher antibacterial activity of MOX loaded into SLN1 is related to the smaller size of SLN1 and distinct lipid and surfactant features, as earlier studies suggest that lipid nanoparticles with Tween 80 can generate higher antibacterial activity against *E. coli* (42). Furthermore, SLN1 can carry MOX directly to the target within the bacterium and also act as efflux pump inhibitor, that is, inhibit drug clearance from the cell (14, 48).

Nanoparticle cytotoxicity

None of the nanoparticles, whether loaded with MOX or not, lowered RAW 264.7 cell viability below 50 % after 24, 48, and 72 h of exposure to all studied concentrations. The highest concentration of standard MOX (not loaded into nanoparticles), however did lower cell viability below 50 %. Our findings therefore suggest that lipid nanoparticles in addition to having low cytotoxicity improve lower the cytotoxicity of MOX and lower its biocompatibility.

Similar observations of nanocarriers lowering MOX cytotoxicity were reported by several studies (49–51).

CONCLUSION

By combining emulsifiers and lipids we successfully prepared stable SLNs and NLCs with high encapsulation efficiency for MOX. These newly designed lipid carriers offered better delivery of the drug into *E. coli* ATCC 25922 compared to the standard MOX formulation, and showed acceptable cytotoxicity and even protection from cytotoxic effects of MOX on RAW 264.7 cells. This finding, however, calls for further investigation and verification in other cell models.

Our findings show that MOX-loaded nanoparticles hold promise as potent chemotherapeutic drugs against *E. coli*. The most promising formulation is SLN1, as it has shown the best results with bacterial uptake and comparable antibacterial activity to MOX at much lower concentration.

Conflict of interests

None to declare.

Acknowledgments

We thank Professor Hande Sipahi from Yeditepe University Faculty of Pharmacy, Department of Pharmaceutical Toxicology for her assistance in providing RAW 264.7 cells.

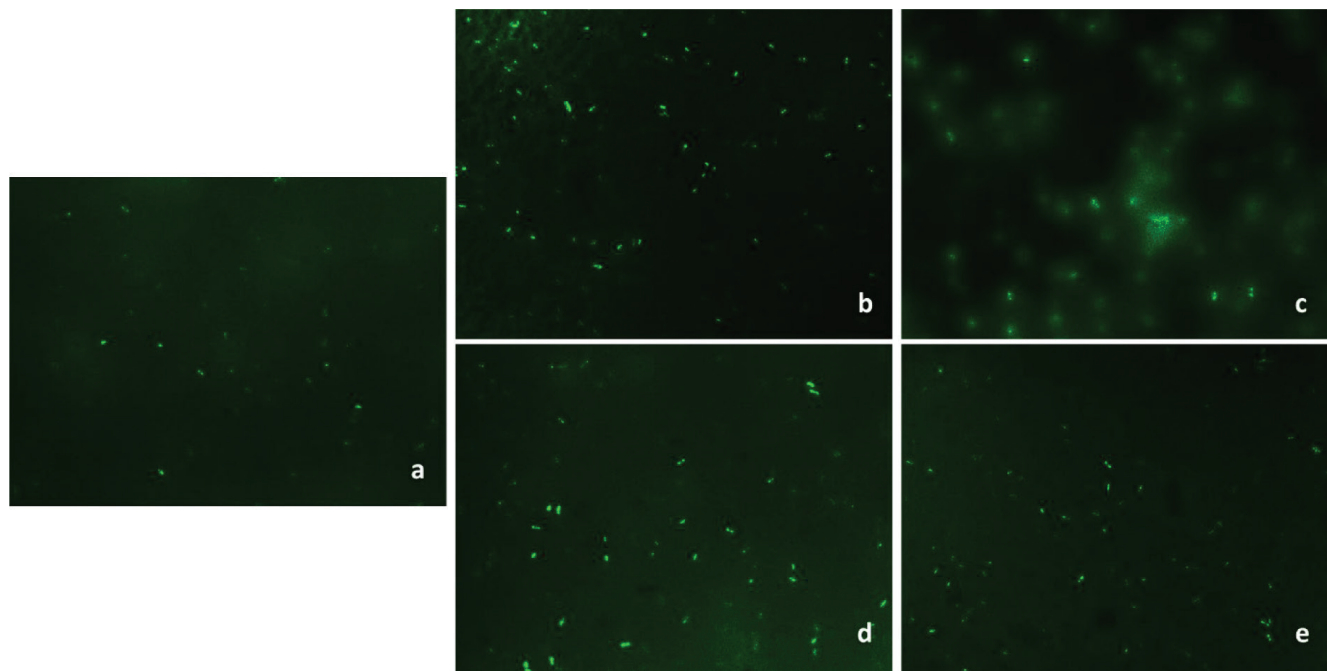


Figure 4 Photomicrographs show bacterial uptake of formulations (a: fluorescein solution; b: SLN1; c: SLN2; d: NLC1; e: NLC2)(40× magnification)

REFERENCES

- Martinez JL, Baquero F. Mutation frequencies and antibiotic resistance. *Antimicrob Agents Chemother* 2000;44:1771–7. doi: 10.1128/AAC.44.7.1771-1777.2000
- Boto L, Martinez JL. Ecological and temporal constraints in the evolution of bacterial genomes. *Genes (Basel)* 2011;2:804–28. doi: 10.3390/genes2040804
- Mackenzie JS, Jeggo M. The one health approach - why is it so important? *Trop Med Infect Dis* 2019;4(2):88. doi: 10.3390/tropicalmed4020088
- Martinez JL. General principles of antibiotic resistance in bacteria. *Drug Discov Today Technol* 2014;11:33–9. doi: 10.1016/j.ddtec.2014.02.001
- World Health Organization (WHO). Antibiotic Resistance [displayed 15 March 2022]. Available at <https://www.who.int/news-room/fact-sheets/detail/antibiotic-resistance>
- Yeh YC, Huang TH, Yang SC, Chen CC, Fang JY. Nano-based drug delivery or targeting to eradicate bacteria for infection mitigation: a review of recent advances. *Front Chem* 2020;8:286. doi: 10.3389/fchem.2020.00286
- Sofowora A, Ogunbodede E, Onayade A. The role and place of medicinal plants in the strategies for disease prevention. *Afr J Tradit Complement Altern Med* 2013;10:210–29. doi: 10.4314/ajtcam.v10i5.2
- Chen CH, Lu TK. Development and challenges of antimicrobial peptides for therapeutic applications. *Antibiotics (Basel)* 2020;9(1):24. doi: 10.3390/antibiotics9010024
- Jiang Q, Chen J, Yang C, Yin Y, Yao K. Quorum sensing: a prospective therapeutic target for bacterial diseases. *Biomed Res Int* 2019;2019:2015978. doi: 10.1155/2019/2015978
- Lin DM, Koskella B, Lin HC. Phage therapy: an alternative to antibiotics in the age of multi-drug resistance. *World J Gastrointest Pharmacol Ther* 2017;8:162–73. doi: 10.4292/wjgpt.v8.i3.162
- Gebreyohannes G, Nyerere A, Bii C, Sbhathu DB. Challenges of intervention, treatment, and antibiotic resistance of biofilm-forming microorganisms. *Heliyon* 2019;5(8):e02192. doi: 10.1016/j.heliyon.2019.e02192
- Arana L, Gallego I, Alkorta I. Incorporation of antibiotics into solid lipid nanoparticles: a promising approach to reduce antibiotic resistance emergence. *Nanomaterials (Basel)* 2021;11(5):1251. doi: 10.3390/nano11051251
- Duan Y, Dhar A, Patel C, Khimani M, Neogi S, Sharma P, Kumar NS, Vekariya RL. A brief review on solid lipid nanoparticles: part and parcel of contemporary drug delivery systems. *RSC Adv* 2020;10:26777–91. doi: 10.1039/D0RA03491F
- Marslin G, Revina AM, Khandelwal VK, Balakumar K, Sheeba CJ, Franklin G. PEGylated ofloxacin nanoparticles render strong antibacterial activity against many clinically important human pathogens. *Colloids Surf B Biointerfaces* 2015;132:62–70. doi: 10.1016/j.colsurfb.2015.04.050
- Sheeba CJ, Marslin G, Revina AM, Franklin G. Signaling pathways influencing tumor microenvironment and their exploitation for targeted drug delivery. *Nanotechnol Rev* 2014;3:123–51. doi: 10.1515/ntrev-2013-0032
- Naseri N, Valizadeh H, Zakeri-Milani P. Solid lipid nanoparticles and nanostructured lipid carriers: structure, preparation and application. *Adv Pharm Bull* 2015;5:305–13. doi: 10.15171/apb.2015.043
- Škalko-Basnet N, Vanić Ž. Lipid-based nanopharmaceuticals in antimicrobial therapy. In: Boukherroub R, Szunerits S, Drider D, editors. *Functionalized nanomaterials for the management of microbial infection*. London: Elsevier; 2017. p. 111–52.

18. Severino P, De Hollanda LM, Santini A, Reis LV, Souto SB, Souto EB, Silva MA. Advances in nanobiomaterials for oncology nanomedicine. In: Grumezescu AM, editor. Nanobiomaterials in cancer therapy: Applications of nanobiomaterials. Vol. 7. Chapter 4. New York (NY): William Andrew Publishing; 2016. p. 91–115.
19. Madkhali OA. Perspectives and prospective on solid lipid nanoparticles as drug delivery systems. *Molecules* 2022;27(5):1543. doi: 10.3390/molecules27051543
20. Esim O, Hascicek C. Lipid-coated nanosized drug delivery systems for an effective cancer therapy. *Curr Drug Deliv* 2021;18:147–61. doi: 10.2174/1567201817666200512104441
21. Elmowafy M, Al-Sanea MM. Nanostructured lipid carriers (NLCs) as drug delivery platform: advances in formulation and delivery strategies. *Saudi Pharm J* 2021;29:999–1012. doi: 10.1016/j.jsps.2021.07.015
22. Misra S, Chopra K, Sinha VR, Medhi B. Galantamine-loaded solid-lipid nanoparticles for enhanced brain delivery: preparation, characterization, *in vitro* and *in vivo* evaluations. *Drug Deliv* 2016;23:1434–43. doi: 10.3109/10717544.2015.1089956
23. Yasir M, Sara UVS. Solid lipid nanoparticles for nose to brain delivery of haloperidol: *in vitro* drug release and pharmacokinetics evaluation. *Acta Pharm Sin B* 2014;4:454–63. doi: 10.1016/j.apsb.2014.10.005
24. Uner M. Preparation, characterization and physico-chemical properties of solid lipid nanoparticles (SLN) and nanostructured lipid carriers (NLC): their benefits as colloidal drug carrier systems. *Pharmazie* 2006;61:375–86. PMID: 16724531
25. The National Center for Biotechnology Information (NCBI). PubChem Compound Summary for CID 152946, Moxifloxacin [displayed 15 March 2022]. Available at <https://pubchem.ncbi.nlm.nih.gov/compound/Moxifloxacin>
26. Guay DR. Moxifloxacin in the treatment of skin and skin structure infections. *Ther Clin Risk Manag* 2006;2:417–34. doi: 10.2147/term.2006.2.4.417
27. Scholar E. Levofloxacin. In: Enna SJ, Bylund DB, editors. *xPharm: The Comprehensive Pharmacology Reference*. New York (NY): Elsevier; 2007. p. 1–6.
28. Wu D, Ding Y, Yao K, Gao W, Wang Y. Antimicrobial resistance analysis of clinical *Escherichia coli* isolates in neonatal ward. *Front Pediatr* 2021;9:670470. doi: 10.3389/fped.2021.670470
29. Pinto-Alphandary H, Andreumont A, Couvreur P. Targeted delivery of antibiotics using liposomes and nanoparticles: research and applications. *Int J Antimicrob Agents* 2000;13:155–68. doi: 10.1016/S0924-8579(99)00121-1
30. Wong JP, Cherwonogrodzky JW, Di Ninno VL, De la Cruz R, Saravolac EG. Liposome-encapsulates ciprofloxacin for the prevention and treatment of infectious diseases caused by intracellular pathogens. In: Shek PN, editor. *Liposomes in biomedical applications*. Amsterdam: Harwood Academic Publishers; 1995. p. 105–20.
31. Mussi SV, Sawant R, Perche F, Oliveira MC, Azevedo RB, Ferreira LA, Torchilin VP. Novel nanostructured lipid carrier co-loaded with doxorubicin and docosahexaenoic acid demonstrates enhanced *in vitro* activity and overcomes drug resistance in MCF-7/Adr cells. *Pharm Res* 2014;31:1882–92. doi: 10.1007/s11095-013-1290-2
32. Topal GR, Kiymaci ME, Özkan Y. Preparation and *in vitro* characterization of vancomycin loaded PLGA nanoparticles for the treatment of *Enterococcus faecalis* infections. *J Fac Pharm Ankara* 2022;46:350–63. doi: 10.33483/jfpau.1073081
33. Yurtdaş Kırımloğlu G, Özer S, Büyükköroğlu G, Yazan Y. Formulation and *in vitro* evaluation of moxifloxacin hydrochloride-loaded polymeric nanoparticles for ocular application. *Lat Am J Pharm* 2018;37:1850–62.
34. Savaser A, Esim O, Kurbanoglu S, Ozkan SA, Özkan Y. Current perspectives on drug release studies from polymeric nanoparticles. In: Grumezescu AM, editors. *Organic materials as smart nanocarriers for drug delivery*. New York (NY): William Andrew Publishing; 2018. p. 101–45.
35. The European Committee on Antimicrobial Susceptibility Testing (EUCAST). Breakpoint tables for interpretation of MICs and zone diameters version 12.0, valid from 2022-01-01 [displayed 15 March 2022]. Available at https://www.eucast.org/fileadmin/src/media/PDFs/EUCAST_files/Breakpoint_tables/v_12.0_Breakpoint_Tables.pdf
36. Bacanlı M, Esim MO, Erdogan H, Sarper M, Erdem O, Özkan Y. Evaluation of cytotoxic and genotoxic effects of paclitaxel-loaded PLGA nanoparticles in neuroblastoma cells. *Food Chem Toxicol* 2021;154:112323. doi: 10.1016/j.fct.2021.112323
37. Sarwar A, Katas H, Zin NM. Antibacterial effects of chitosan-tripolyphosphate nanoparticles: impact of particle size molecular weight. *J Nanoparticle Res* 2014;16:2517. doi: 10.1007/s11051-014-2517-9
38. Martins S, Tho I, Reimold I, Fricker G, Souto E, Ferreira D, Brandl M. Brain delivery of camptothecin by means of solid lipid nanoparticles: formulation design, *in vitro* and *in vivo* studies. *Int J Pharm* 2012;439:49–62. doi: 10.1016/j.ijpharm.2012.09.054
39. Schöler N, Olbrich C, Tabatt K, Müller RH, Hahn H, Liesenfeld O. Surfactant, but not the size of solid lipid nanoparticles (SLN) influences viability and cytokine production of macrophages. *Int J Pharm* 2001;221:57–67. doi: 10.1016/S0378-5173(01)00660-3
40. Lages EB, Fernandes RS, Silva JO, de Souza AM, Cassali GD, de Barros ALB, Miranda Ferreira LA. Co-delivery of doxorubicin, docosahexaenoic acid, and alpha-tocopherol succinate by nanostructured lipid carriers has a synergistic effect to enhance antitumor activity and reduce toxicity. *Biomed Pharmacother* 2020;132:110876. doi: 10.1016/j.biopha.2020.110876
41. Das S, Ng WK, Kanaujia P, Kim S, Tan RB. Formulation design, preparation and physicochemical characterizations of solid lipid nanoparticles containing a hydrophobic drug: effects of process variables. *Colloids Surf B Biointerfaces* 2011;88:483–9. doi: 10.1016/j.colsurfb.2011.07.036
42. Amasya G, Bakar-Ates F, Wintgens V, Amiel C. Layer by layer assembly of core-corona structured solid lipid nanoparticles with beta-cyclodextrin polymers. *Int J Pharm* 2021;592:119994. doi: 10.1016/j.ijpharm.2020.119994
43. Singh S, Dobhal AK, Jain A, Pandit JK, Chakraborty S. Formulation and evaluation of solid lipid nanoparticles of a water soluble drug: Zidovudine. *Chem Pharm Bull (Tokyo)* 2010;58:650–5. doi: 10.1248/cpb.58.650
44. Al-Qushawi A, Rassouli A, Atyabi F, Peighambari SM, Esfandyari-Manesh M, Shams GR, Yazdani A. Preparation and characterization of three tilmicosin-loaded lipid nanoparticles: physicochemical properties and *in-vitro* antibacterial activities. *Iran J Pharm Res* 2016;15:663–76. PMID: PMC5316245
45. Müller RH, Radtke M, Wissing SA. Nanostructured lipid matrices for improved microencapsulation of drugs. *Int J Pharm* 2002;242:121–8. doi: 10.1016/S0378-5173(02)00180-1
46. Ebrahimi S, Farhadian N, Karimi M, Ebrahimi M. Enhanced bactericidal effect of ceftriaxone drug encapsulated in nanostructured

- lipid carrier against gram-negative *Escherichia coli* bacteria: drug formulation, optimization, and cell culture study. *Antimicrob Resist Infect Control* 2020;9(1):28. doi: 10.1186/s13756-020-0690-4
47. Kumar S, Bhanjana G, Kumar A, Taneja K, Dilbaghi N, Kim KH. Synthesis and optimization of ceftriaxone-loaded solid lipid nanocarriers. *Chem Phys Lipids* 2016;200:126–32. doi: 10.1016/j.chemphyslip.2016.09.002
48. Esim O, Sarper M, Ozkan CK, Oren S, Baykal B, Savaser A, Ozkan Y. Effect simultaneous delivery with P-glycoprotein inhibitor and nanoparticle administration of doxorubicin on cellular uptake and *in vitro* anticancer activity. *Saudi Pharm J* 2020;28:465–72. doi: 10.1016/j.jsps.2020.02.008
49. Akbar N, Gul J, Siddiqui R, Shah MR, Khan NA. Moxifloxacin and sulfamethoxazole-based nanocarriers exhibit potent antibacterial activities. *Antibiotics (Basel)* 2021;10(8):964. doi: 10.3390/antibiotics10080964
50. Kisich KO, Gelperina S, Higgins MP, Wilson S, Shipulo E, Oganessian E, Heifets L. Encapsulation of moxifloxacin within poly(butyl cyanoacrylate) nanoparticles enhances efficacy against intracellular *Mycobacterium tuberculosis*. *Int J Pharm* 2007;345:154–62. doi: 10.1016/j.ijpharm.2007.05.062
51. Tshweu LL, Shemis MA, Abdelghany A, Gouda A, Pilcher LA, Sibuyi NR, Meyer M, Dube A, Balogun MO. Synthesis, physicochemical characterization, toxicity and efficacy of a PEG conjugate and a hybrid PEG conjugate nanoparticle formulation of the antibiotic moxifloxacin. *RSC Adv* 2020;10:19770–80. doi: 10.1039/C9RA10872F

Ocjena apsorpcije, djelotvornosti protiv bakterije *Escherichia coli* i citotoksičnosti krutih lipidnih nanočestica s moksifloksacinom

Moksifloksacin je važan antibiotik koji se često rabi za liječenje rekurentne infekcije bakterijom *Escherichia coli* (*E. coli*). Cilj je ovog istraživanja bio ocijeniti njegovu djelotvornost u formulaciji s krutim lipidnim nanočesticama (engl. *solid lipid nanoparticles*, krat. SLN) i nanostrukturiranim lipidnim nosačima (engl. *nanostructured lipid carriers*, krat. NLC) kao njegovim vehikulima. U tu smo svrhu osmislili dva SLN-a (SLN1 i SLN2) te dva NLC-a (NLC1 i NLC2) različitih svojstava (veličine čestice, raspodjele veličina, zeta potencijala i sposobnosti enkapsulacije) te ih obogatili moksifloksacinom kako bismo utvrdili njegovo otpuštanje, djelovanje protiv *E. coli* i citotoksičnost za makrofagnu staničnu liniju RAW 264.7 *in vitro*. S bakterijskom apsorpcijom od 57,29 %, SLN1 se pokazao značajno djelotvornijim vehikulom moksifloksacina od njegove standardne formulacije (otopine), a formulacije s SLN2, NLC1 odnosno NLC2 s odgovarajućim apsorpcijama od 50,74 %, 39,26 % odnosno 32,79 % iskazale su djelotvornost sličnu onoj standardnog antibiotika. Test citotoksičnosti nije pokazao značajnu toksičnost nanočestica bez obzira na to jesu li sadržavale moksifloksacin ili nisu. Naši rezultati upućuju na mogući smjer razvoja djelotvornih lipidnih nosača kojima bi se mogle smanjiti nuspojave i povećati antibakterijska djelotvornost liječenja s obzirom na sve veću bakterijsku rezistentnost.

KLJUČNE RIJEČI: antibiotik; biokompatibilnost; *E. coli*; nanočestice s lipidima; rezistentnost na lijek; stanična linija RAW 264.7